

Observation of Cell Passing through Single Micro Slit between Weir-walls

Shigehiro HASHIMOTO, Yusuke TAKAHASHI, Yusuke NAKANO,
Daisuke HASEGAWA, Yuki TAKIGUCHI

Biomedical Engineering, Department of Mechanical Engineering,
Kogakuin University, Tokyo, 163-8677, Japan
shashimoto@cc.kogakuin.ac.jp <http://www.mech.kogakuin.ac.jp/labs/bio/>

and

Toshitaka YASUDA

Bio-systems Engineering, Department of Electronic Engineering,
Tokyo National College of Technology, Tokyo, Japan

ABSTRACT

The single micro slits of two kinds of width (10 μm , or 15 μm) has been designed between weir-walls to investigate the deformation of a cell passing through the slit related to the flow rate *in vitro*. The micro slit (0.1 mm length, and 55 μm height) was fabricated between weir-walls of polydimethylsiloxane using the micromachining technique. The single micro slit is set in the flow path (2 mm width, 55 μm height) between parallel plates. Two types of biological cells were used in the test alternatively: C2C12 (mouse myoblast cell), and Hepa1-6 (mouse hepatoma cell). The suspension of cells was introduced into the slits by the pressure difference between the inlet and the outlet, which was kept by the gravitational level difference of the medium (< 4 mm). The each flowing cell was observed by an inverted phase contrast microscope. The movement and the shape of the cell was analyzed at the video images by the camera at the eyepiece of the microscope. The experimental results shows that some myoblasts pass the slit at the higher deformation ratio with the higher flow rate. The experimental results show that the designed slit has capability to measure deformability of the cell.

Keywords: Biomedical Engineering, C2C12, Hepa1-6, Deformation, Micromachining and Micro Slit.

1. INTRODUCTION

Biological cells can pass through narrow gaps: micro capillaries, or micro slits. The biological system sorts cells according to the size, deformability, and adsorptivity of the cell. Cells are sorted according to deformability through the gap or adsorptivity on the membrane *in vitro* [1-17]. The technique might be applied to handle cells in diagnostics *in vitro* [13-17].

The photolithography technique enables manufacturing a micro-pattern [18-21]. Several micro-fabrication processes have been designed to simulate the morphology of the

microcirculation. In the previous study, the micro slits have designed between micro cylindrical pillars [1], or between micro ridges [2]. The micro-fabrication technique has also been applied to design microfluidic systems *in vitro* [3-16].

To analyze mechanical property of deformation of the single cell, the single slit has an advantage than parallel arrangement of slits. With the parallel slits, the flow rate through each slit cannot be maintained at constant value.

In the present study, the single micro slits of two kinds of width (0.010 mm, or 0.015 mm) has been designed between weir-walls to investigate the deformation of a cell passing through the slit related to the flow rate *in vitro*.

2. METHODS

Micro Slit

A single micro slit has been fabricated between weir-walls on the glass plate using the photolithography technique: 0.1 mm length (L) and 0.055 mm height (H). Variation was made on the width of the slit: 0.010 mm, and 0.015 mm. The single micro slit was set in the flow path between parallel polydimethylsiloxane (PDMS) plates, of which dimension of the cross section has 2 mm width (W), 30 mm length and 0.055 mm height (H). The upper plate has two holes of 5 mm diameter for the inlet and for the outlet of the flow of the cell suspension. The upper plate with the micro slit was made by two kinds of molds, which were made by the following process.

Photomask

The slide glass (Matsunami) plate (38 mm length, 26 mm width, and 1.0 mm thickness) was used for the base of the photomask (Fig. 1). Before the deposition of titanium, the surface of the glass plate was hydrophilized by the oxygen (30 cm^3/min , 0.1 Pa) plasma ashing for five minutes at 100 W by the reactive ion etching system (FA-1, Samco International, Kyoto, Japan). Titanium was deposited on the surface of the glass plate with

200 nm thickness in the sputtering system (back pressure 9×10^{-4} Pa, RF100W, 0.5 Pa, 8 min, L-210S-FH Canon Anelva Corporation, Kawasaki, Japan). The oxygen (0.1 Pa, 30 cm³/min) ashing was applied on the surface of the titanium in the reactive ion etching system (RF 100 W, for five minutes, FA-1).

To improve affinity to photoresist material, HMDS (hexamethyldisilazane: Tokyo Chemical Industry Co., Ltd., Tokyo) was coated on the glass plate at 3000 rpm for 30 s with a spin coater. The positive photoresist material of OFPR-800LB (Tokyo Ohka Kogyo Co., Ltd, Tokyo, Japan) was coated on the titanium with the spin coater (at 7000 rpm for 30 s). The photoresist was baked in the oven (DX401, Yamato Scientific Co., Ltd) at 373 K for one minute.

The pattern for the slit was drawn on the mask with a laser drawing system (DDB-201K-KH, Neoark Corporation, Hachioji, Japan). To control the dimension of the pattern on the mold with the laser drawing system, the parameters were selected as follows: the voltage of 3.05 V, the velocity of 0.137 mm/s, the acceleration of 0.5 mm/s², and the focus offset at +2.4.

The photoresist was developed with tetra-methyl-ammonium hydroxide (NMD-3, Tokyo Ohka Kogyo Co., Ltd., Kawasaki, Japan) for one minute, rinsed with the distilled water (300 rpm, 30 s), and dried by the spin-dryer (1100 rpm, 30 s, with N₂ gas, SF-250, Japan Create Co., Ltd., Tokorozawa, Japan).

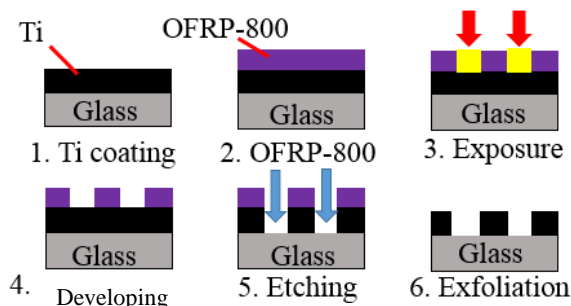


Fig. 1: Photolithography process for photomask.

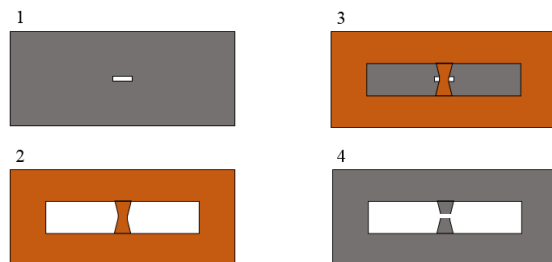


Fig. 2: Polyimide tape was pasted over slit position.

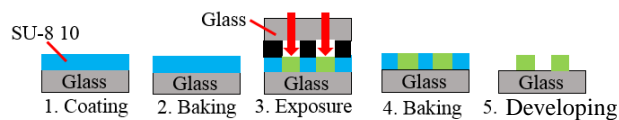


Fig. 3: Mold A.

The titanium coated plate was etched with the plasma gas using RIE-10NR (Samco International, Kyoto, Japan). For etching, the gas of SF₆ (50 cm³/min at 1013 hPa) with Ar (50 cm³/min at 1013 hPa) was applied at 100 W at 4 Pa for four minutes. The residual OFPR-800LB was removed by acetone. The plate was dipped in the distilled water in one minute, after it is dipped in ethanol for one minute. The plate was dried by the spin-dryer: 300 rpm for 30 s with the distilled water, and 1100 rpm for 30 s with N₂ gas.

The polyimide tape (0.055 mm thickness, 10 mm width), which was cut to make the channel by the ultra-short pulse laser (IFRIT, Cyber Laser Inc., Tokyo, Japan), was pasted over the slit position at the center of the glass plate (Fig. 2). The titanium coated plate was etched again with the plasma gas using RIE-10NR. For etching, the gas of SF₆ (50 cm³/min at 1013 hPa) with Ar (50 cm³/min at 1013 hPa) was applied at 100 W at 4 Pa for four minutes.

Mold A

The slide glass (Matsunami) plate (38 mm length, 26 mm width, and 1.0 mm thickness) was used for the base of the mold, after cleaning for three minutes with an ultrasonic cleaning machine (Fig. 3). The plate was dried by the spin-dryer: 300 rpm for 30 s with the distilled water, and 1100 rpm for 30 s with N₂ gas. The surface of the glass plate was hydrophilized by the oxygen (30 cm³/min, 0.1 Pa) plasma ashing for five minutes at 100 W by the reactive ion etching system (FA-1).

The epoxy based negative photoresist material (SU-8 100) was coated on the glass with the spin coater (at 3000 rpm for 30 s). The photoresist was baked in the oven (DX401) at 338 K for ten minutes and at 368 K for one hour.

The photoresist was exposed to the UV light through the photomask in the mask aligner (M-1S, Mikasa Co. Ltd., Japan) at 16.2 mW/cm² for 30 s. The photoresist was baked in the oven at 338 K for one minute, and at 368 K for five minutes. The photoresist was developed with SU-8 developer (Micro Chem Corp., MA, USA) for ten minutes. The glass surface with the micro pattern was rinsed with IPA (2-propanol, Wako Pure Chemical Industries, Ltd.) for one minute, and pure water for one minute. The pattern was baked for five minutes in the oven at 393 K.

Mold B

The slide glass (Matsunami) plate (38 mm length, 26 mm width, and 1.0 mm thickness) was used for the base of the mold (Fig. 4). The polyimide tape (0.055 mm thickness, 10 mm width) was pasted at the center of the glass plate. The tape was cut by the ultra-short pulse laser (IFRIT) to make the mold for the upper part of the flow channel with the single slit. The dimension of the slit on the manufactured mold was measured with the laser microscope (VK-X200, Keyence Corporation, Osaka, Japan). The height along the cross sectional line of the slit was traced.

Upper Plate

After the mold of the slide glass plate was enclosed with a peripheral wall of polyimide tape, PDMS (Sylgard 184 Silicone Elastomer Base, Dow Corning Corp., MI, USA) was poured with the curing agent (Sylgard 184 Silicone Elastomer Curing Agent, Dow Corning Corp., MI, USA) on the mold (Fig. 5). The volume ratio of PDMS to curing agent is ten to one.

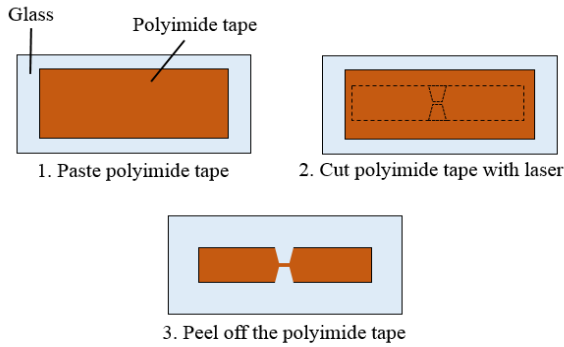


Fig. 4: Mold B.

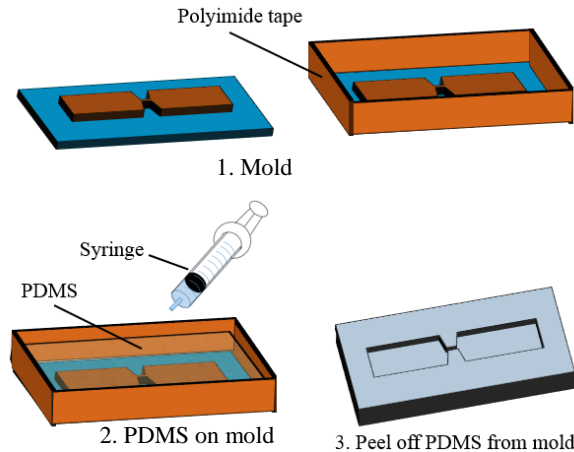


Fig. 5: Upper plate with slit.

After degassing, PDMS was baked at 368 K for 15 min in an oven (DX401, Yamato Scientific Co., Ltd). The baked plate of PDMS (4 mm thickness) was exfoliated from the mold of the slide glass plate. The PDMS plate was cut to make a rectangular upper plate for the flow channel. Two holes (diameter of 5 mm) with the interval of 25 mm were punched by a punching tool (trepan MK405, Kai Industries Co., Ltd., Gifu, Japan) to make the inlet and the outlet. The morphology of the slit was observed by a scanning electron microscope (SEM, JSM6360LA, JEOL Ltd., Tokyo, Japan).

Lower Plate

The slide glass plate (38 mm length, 26 mm width, and 1.0 mm thickness) was used for the base of the lower plate. PDMS was coated on the glass plate at 5000 rpm for one minute with the spin coater, and baked in the oven at 368 K for ten minutes. The surface of the lower plate was hydrophilized by the oxygen (30 cm³/min, 0.1 Pa) plasma ashing for one minute at 100 W by the reactive ion etching system (FA-1).

Flow Channel

By the surface affinity, the upper plate was stuck on the lower plate to make the flow channel. A rectangular parallelepiped channel of 30 mm length × 2 mm width × 0.05 mm height is formed between upper and lower plates. The two plates stick together with their surface affinity.

The flow channel is placed on the stage of the inverted phase contrast microscope (IX71, Olympus Co., Ltd., Tokyo) (Fig. 6).

Flow Test

Cells of the passage between four and nine were used in the test.

Two types of biological cells were used in the test alternatively: C2C12 (mouse myoblast cell line originated with cross-striated muscle of C3H mouse), or Hepa1-6 (mouse hepatoma cell line of C57L mouse). The inner surface of the flow channel was hydrophilized by the oxygen (30 cm³/min, 0.1 Pa) plasma ashing for one minute at 100 W by the reactive ion etching system (FA-1, Samco International, Kyoto, Japan), and pre-filled with the bovine serum albumin solution for thirty minutes at 310 K.

Before the flow test, the cells were exfoliated from the plate of the culture dish with trypsin, and suspended in the D-MEM (Dulbecco's Modified Eagle's Medium). The suspension of cells (80 mm³) was poured at the inlet of the flow channel. The flow occurs by the pressure difference between the inlet and the outlet, which was kept by the gravitational level of the medium (< 3 mm).

The cell passing through the slit was observed by the microscope, and recorded by the camera (DSC-RX100M4, Sony Corporation, Japan), which is set at the eyepiece of the microscope. The movement of the cell was analyzed by "Kinovea (Ver. 8.23, Commons Attribution)" at the video images: 30 frames per second. At the images, the outline of each cell was traced with "Image J (Ver. 1.48, National Institutes of Health)", and the diameter (D_0) was calculated.

The deformation of the cell in the slit was evaluated by the following equations (Fig. 7).

$$Q = vA = v(bH) \quad (1)$$

$$\varepsilon = (D_0 - D_1) / D_0 \quad (2)$$

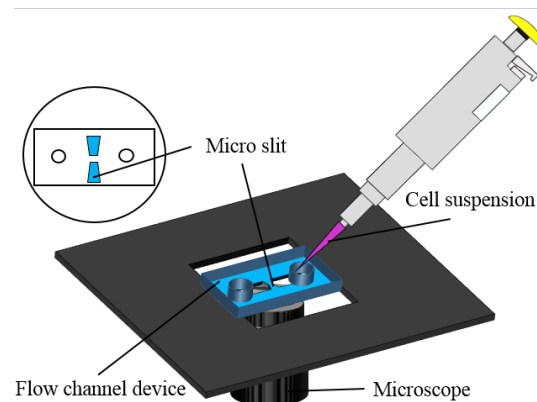


Fig. 6: Flow channel is placed on stage of inverted phase contrast microscope.

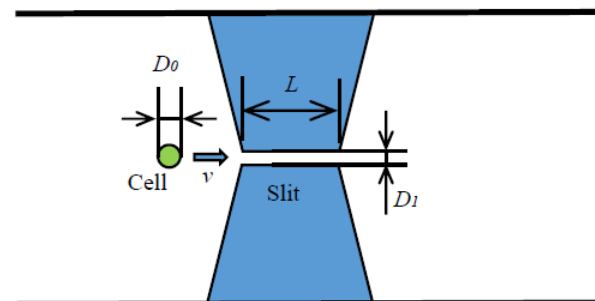


Fig. 7: Schematic image of cross section of slit.

Where Q is the flow rate in the channel, v is the flow velocity before the slit, A is the cross sectional area of the channel, H is the height of the slit (5×10^{-5} m), b is the width of the flow channel (2 mm), D_0 is the initial diameter of the cell, D_1 is the width of the slit, and ε is the strain of the cell.

3. RESULTS

Fig. 8 shows the tracings of the surface of the tape on the glass for the mold of slit by the laser microscope. The dimension (0.010 mm width) of the mold was confirmed at the tracings. The designed pattern is successfully machined at the polyimide tape pasted on the glass. Fig. 9 shows the scanning electron microscope image of the slit between weir-walls. The image shows the approximately rectangular groove. The top opening side of the groove is covered by the counter plate to make the slit. Fig. 10 exemplifies the microscopic image of C2C12 passing through the slit. The cell approaches to the slit (Fig. 10a), enters in the slit (Fig. 10b), moves through the slit (Fig. 10c), and moves away from the slit (Fig. 10d).

Fig. 11 exemplifies the velocity of C2C12 passing through the slit. The zero velocity corresponds to the movement of the cell clogging in the slit. The term of 1.3 s between two peaks correspond to the term of the cell passing through the slit. Fig. 12 shows the relationship between the flow rate and the strain of each cell, which passes through the slit. In Fig. 12, datum of the circle corresponds to that of C2C12, and datum of the triangle corresponds to that of Hepa1-6. The data group of the lower strain correspond to data at the wider slit of 0.015 mm width, and the data group of the higher strain correspond to data at the narrower slit of 0.010 mm. Hepa1-6 does not pass through the slit of 0.010 mm width. Some myoblasts pass the slit of 0.010 mm width at the higher deformation ratio with the higher flow rate. There is positive correlation between flow rate and deformation ratio at C2C12. At the wider slit of 0.015 mm width, on the other hand, even the cell of the bigger diameter passes through the slit at the lower flow rate.

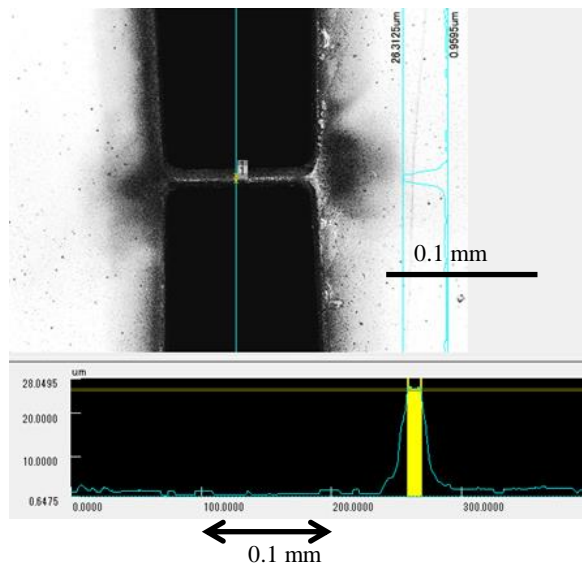


Fig. 8: Tracings (lower) along the blue line (upper) of surface of tape on glass for mold of slit by laser microscope: unit, μm .

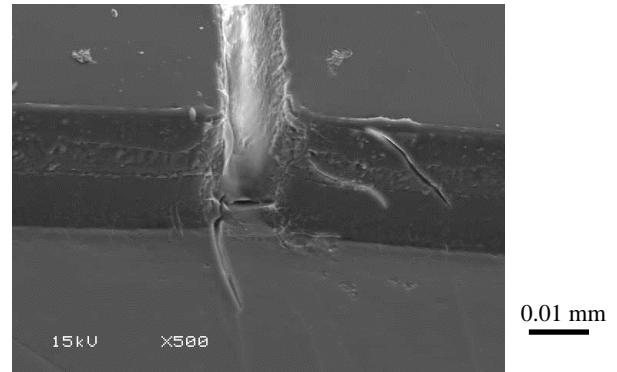


Fig. 9: SEM image of slit. Dimension from left to right is 0.1 mm.



Fig. 10a: C2C12 (marked by the circle) approaching to slit: flow from left to right, dimension from left to right is 0.5 mm.



Fig. 10b: C2C12 passing through slit.



Fig. 10c: C2C12 passing through slit.



Fig. 10d: C2C12 moves away from the slit.

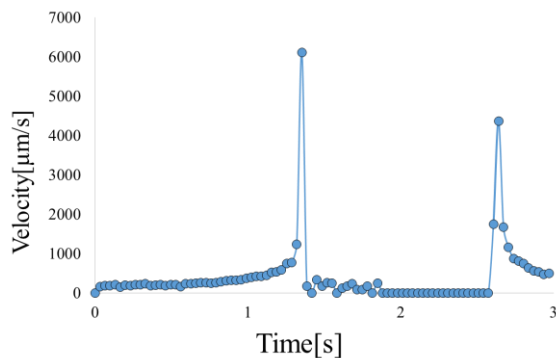


Fig. 11: Velocity of C2C12 passing through slit.

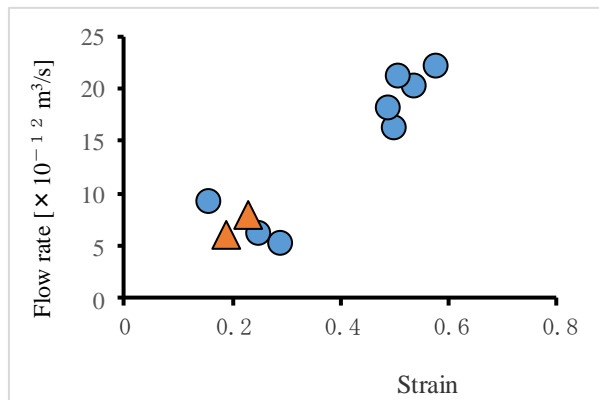


Fig. 12: Flow rate vs. strain of C2C12 (circle) and Hepa1-6 (triangle) passing through slit.

4. DISCUSSION

Preparation of the slit of sub-micrometer is not easy. In the previous study, the slit of micrometer between pillars was manufactured by photolithography technique [1]. Only one projection can be traced in the present experimental system. The cell deforms in the three dimensional space. To observe the deformation in the perpendicular plane, the slit between upper and lower ridges is effective [2].

In the present study, the slit of the narrow width (0.010 mm, and 0.015 mm) has been machined by micromachining technique: the ultra-short pulse laser, or photolithography. The results of the dimension of the machining was acceptable for the slit, where the movement of each cell was able to be observed. Two kinds of dimension of the width of the slit enable the wider range of the strain in the experiment. At the narrower slit, the higher flow rate is necessary for the bigger cell (bigger diameter,

higher strain) to pass through the slit (Fig. 12). The deformation of the harder part of the cell might be necessary to pass through the narrower slit.

There are several methods to sort cells [1-12]. Non-invasive way is preferable to sort cells with minimum damage. The flow cytometry is one of the technologies, which is used for cell sorting. Cells suspended in the fluid are analyzed by the laser. The fluorescently labelled components in the cell are analyzed by the light emission. The experimental results might contribute to analyze adhesive mechanism of cancer cell during metastasis. The micro trap might simulate adhesive mechanism of flowing cells.

A red blood cell has flexibility and deforms in the shear flow [22, 23]. It also passes through micro-circulation, of which the dimension is smaller than the diameter of the red blood cell. After circulation through the blood vessels for days, the red blood cell is trapped in the micro-circulation systems. Cells has deformability [24], and some cells can pass through the slit narrower than the capillary.

In the previous study, several slits were designed between micro columns [1]. The multiple slits are convenient to sort cells as the filter. The fluid selects, however, a slit of parallel multiple slits at random. While a cell is passing through a slit, the main fluid flows through another slit. The driving force of the cell passing changes with the clogging at the slit.

The resistance of the flow channel with a single slit is very high in the present experimental system. The resistance increases, when the cells clogged the slits in the flow channel. Internal pressure of the flow channel should be carefully controlled under the constant flow rate, otherwise the leakage or cavitation would occur. The flow path was carefully examined to avoid mixing of air bubbles, which might stir the medium in the flow channel.

In the present study, the flow is controlled by the pressure difference between the inlet and the outlet, which was kept by the gravitational level of the medium. The diameter (5 mm) of the inlet port is much larger than cross sectional area of the slit to keep the level of the inlet port. In the present study, the flow rate is confirmed by the flow speed of the cell during microscopic observation.

The capture of the cell at the slit depends on several factors: the dimension of the cell and the slit, deformability of the cell, the wall shear stress (shear rate) at the slit, and the affinity (charge, friction) of the cell to the wall of the slit. The surface is not completely flat in the slit, which might increase frictional resistance. The wall of the slit has roughness (Fig. 9), which affects the movement of each cell passing through the slit. In the present study, Neuro-2a (a mouse neural crest-derived cell line) tends to adhere to the wall of the flow channel, and is difficult to be observed the movement of passing through the slit. Protein coating might make property of the surface stable.

5. CONCLUSION

The single micro slits of two kinds of width (0.010 mm, or 0.015 mm) has been designed between weir-walls to investigate the deformation of a cell passing through the slit related to the flow rate *in vitro*. The micro slit of 0.1 mm length and 0.05

mm height was fabricated between weir-walls of the polydimethylsiloxane plates using the photolithography technique. The suspension of cells (C2C12 or Hepa1-6) was introduced into the slits, and the cell passing through the slit was observed by the microscope. The experimental results shows that some myoblasts pass through the slit at the higher deformation ratio with the higher flow rate. Both the movement and the shape of the cell were analyzed at the video images. The experimental results show that the designed slit has capability to measure deformability of the cell.

6. ACKNOWLEDGMENT

This work was supported by a Grant-in-Aid for Strategic Research Foundation at Private Universities from the Japanese Ministry of Education, Culture, Sports and Technology.

REFERENCES

- [1] Y. Takahashi, S. Hashimoto, H. Hino and T. Azuma, "Design of Slit between Micro Cylindrical Pillars for Cell Sorting", **Journal of Systemics, Cybernetics and Informatics**, Vol. 14, No. 6, 2016, pp. 8-14.
- [2] Y. Takahashi, S. Hashimoto, A. Mizoi and H. Hino, "Deformation of Cell Passing through Micro Slit between Micro Ridges Fabricated by Photolithography Technique", **Journal of Systemics, Cybernetics and Informatics**, Vol. 15, No. 3, 2017, pp. 1-9.
- [3] Y. Takahashi, S. Hashimoto, A. Mizoi, H. Hino, T. Yamaguchi and T. Yasuda, "Measurement of Deformability of Biological Cell Passing through Single Micro Slit between Walls", **Proc. 21st World Multi-Conference on Systemics Cybernetics and Informatics**, Vol. 2, 2017, pp. 233-238.
- [4] M. Yamada and M. Seki, "Hydrodynamic Filtration for On-chip Particle Concentration and Classification Utilizing Microfluidics", **Lab on a Chip**, Vol. 5, No. 11, 2005, pp. 1233-1239.
- [5] H.M. Ji, V. Samper, Y. Chen, C.K. Heng, T.M. Lim and L. Yobas, "Silicon-based Microfilters for Whole Blood Cell Separation", **Biomedical Microdevices**, Vol. 10, 2008, pp. 251-257.
- [6] Y. Takahashi, S. Hashimoto, H. Hino, A. Mizoi and N. Noguchi, "Micro Groove for Trapping of Flowing Cell", **Journal of Systemics, Cybernetics and Informatics**, Vol. 13, No. 3, 2015, pp. 1-8.
- [7] A. Khademhosseini, J. Yeh, S. Jon, G. Eng, K.Y. Suh, J.A. Burdick and R. Langer, "Molded Polyethylene Glycol Microstructures for Capturing Cells within Microfluidic Channels", **Lab on a Chip**, Vol. 4, No. 5, 2004, pp. 425-430.
- [8] S.M. McFaul, B.K. Lin and H. Ma, "Cell Separation Based on Size and Deformability Using Microfluidic Funnel Ratchets", **Lab on a Chip**, Vol. 12, No. 13, 2012, pp. 2369-2376.
- [9] M. Islam, H. Brink, S. Blanche, C. DiPrete, T. Bongiorno, N. Stone, A. Liu, A. Philip, G. Wang, W. Lam, A. Alexeev, E.K. Waller and T. Sulchek, "Microfluidic Sorting of Cells by Viability Based on Differences in Cell Stiffness", **Scientific Reports**, Vol. 7, No. 1, 2017, pp. 1997-2008.
- [10] S.C. Hur, N.K. Henderson-Maclennan, E.R.B. McCabe and D.D. Carlo, "Deformability-based Cell Classification and Enrichment Using Inertial Microfluidics", **Lab on a Chip**, Vol. 11, No. 5, 2011, pp. 912-920.
- [11] A.A. Bhagat, H. Bow, H.W. Hou, S.J. Tan, J. Han and C.T. Lim, "Microfluidics for Cell Separation", **Medical & Biological & Engineering & Computing**, Vol. 48, No. 10, 2010, pp. 999-1014.
- [12] D.R. Gossett, W.M. Weaver, A.J. Mach, S.C. Hur, H.T.K. Tse, W. Lee, H. Amini and D.D. Carlo, "Label-free Cell Separation and Sorting in Microfluidic Systems", **Analytical and Bioanalytical Chemistry**, Vol. 397, No. 8, 2010, pp. 3249-3267.
- [13] H.W. Hou, Q.S. Li, G.Y.H. Lee, A.P. Kumar, C.N. Ong and C.T. Lim, "Deformability Study of Breast Cancer Cells Using Microfluidics", **Biomedical Microdevices**, Vol. 11, No. 3, 2009, pp. 557-564.
- [14] W. Zhang, K. Kai, D.S. Choi, T. Iwamoto, Y.H. Nguyen, H. Wong, M.D. Landis, N.T. Ueno, J. Chang and L. Qin, "Microfluidics Separation Reveals the Stem-cell-like Deformability of Tumor-initiating Cells", **Proceedings of the National Academy of Science**, Vol. 109, No. 46, 2012, pp. 18707-18712.
- [15] Z. Liu, F. Huang, J. Du, W. Shu, H. Feng, X. Xu and Y. Chen, "Rapid Isolation of Cancer Cells Using Microfluidic Deterministic Lateral Displacement Structure", **Biomicrofluidics**, Vol. 7, No. 1, 2013, pp. 011801-1-10.
- [16] B.K. Lin, S.M. McFaul, C. Jin, P.C. Black and H. Ma, "Highly Selective Biomechanical Separation of Cancer Cells from Leukocytes Using Microfluidic Ratchets and Hydrodynamic Concentrator", **Biomicrofluidics**, Vol. 7, No. 3, 2013, pp. 034114-1-11.
- [17] S.K. Lee, G.S. Kim, Y. Wu, D.J. Kim, Y. Lu, M. Kwak, L. Han, J.H. Hyung, J.K. Seol, C. Sander, A. Gonzalez, J. Li and R. Fan, "Nanowire Substrate-based Laser Scanning Cytometry for Quantitation of Circulating Tumor Cells", **Nano Letters**, Vol. 12, No. 6, 2012, pp. 2697-2704.
- [18] H. Hino, S. Hashimoto and F. Sato, "Effect of Micro Ridges on Orientation of Cultured Cell", **Journal of Systemics Cybernetics and Informatics**, Vol. 12, No. 3, 2014, pp. 47-53.
- [19] H. Hino, S. Hashimoto, Y. Shinozaki, H. Sugimoto and Y. Takahashi, "Effect of Flow on Cultured Cell at Micro-pattern of Ridge Lines", **Journal of Systemics, Cybernetics and Informatics**, Vol. 15, No. 5, 2017, pp. 1-7.
- [20] H. Hino, S. Hashimoto, S. Nishino, Y. Takahashi and H. Sugimoto, "Behavior of Cell on Vibrating Micro Ridges", **Journal of Systemics, Cybernetics and Informatics**, Vol. 13, No. 3, 2015, pp. 9-16.
- [21] J. Friend and L. Yeo, "Fabrication of Microfluidic Devices Using Polydimethylsiloxane", **Biomicrofluidics**, Vol. 4, No. 4, 2010, pp. 26052-26057.
- [22] S. Hashimoto, et al., "Effect of Aging on Deformability of Erythrocytes in Shear Flow", **Journal of Systemics, Cybernetics and Informatics**, Vol. 3, No. 1, 2005, pp. 90-93.
- [23] S. Hashimoto, "Detect of Sublethal Damage with Cyclic Deformation of Erythrocyte in Shear Flow", **Journal of Systemics Cybernetics and Informatics**, Vol. 12, No. 3, 2014, pp. 41-46.
- [24] T. Yokokura, Y. Nakashima, Y. Yonemoto, Y. Hikichi and Y. Nakanishi, "Method for Measuring Young's Modulus of Cells Using a Cell Compression Microdevice", **International Journal of Engineering Science**, 2017, Vol. 114, pp. 41-48.